

**EVOLUTION OF MICROSTRUCTURE OF MAGNESIUM MATERIALS PREPARED BY SPS  
USING VARIOUS COMPACTING PRESSURES**

<sup>1</sup>Roman BRESCHER, <sup>1</sup>Michaela HASONOVÁ, <sup>1</sup>Matěj BŘEZINA, <sup>1,2</sup>Stanislava FINTOVÁ,  
<sup>1,3</sup>Pavel DOLEŽAL, <sup>1</sup>Jaromír WASSERBAUER

<sup>1</sup>*Institute of Materials Science, Faculty of Chemistry BUT, Brno, Czech Republic, EU, [brezina@fch.vut.cz](mailto:brezina@fch.vut.cz)*

<sup>2</sup>*Institute of Physics of Materials, Czech Academy of Sciences, Brno, Czech Republic, EU*

<sup>3</sup>*Institute of Materials Science and Engineering, Faculty of Mechanical Engineering, Brno University of  
Technology, Brno, Czech Republic, EU*

<https://doi.org/10.37904/metal.2022.4500>

**Abstract**

Compacting pressure applied during the SPS method varies in the literature. This study evaluates the influence of the applied compacting pressure on the microstructure and porosity of sintered materials. Using spark plasma sintering (SPS), cold compacted magnesium powder (green compacts) was sintered to bulk magnesium materials. The green magnesium compacts were prepared at room temperature using 100 MPa of uniaxial pressure, which was applied for 60 s. Using SPS, the green compacts sintering was carried out at 400 °C for 10 min. Various compacting pressures were applied during sintering: 20, 40, 60, 80 and 100 MPa to analyse the influence of the pressure. The resulting microstructure and porosity strongly depended on the compacting pressure applied during SPS. An increase of the compacting pressure was shown to be beneficial for material homogeneity, while this effect was pronounced up to 60 MPa, and only a slight effect on the material porosity was observed above this pressure.

**Keywords:** Magnesium, powder metallurgy, SPS, microstructure, porosity

**1. INTRODUCTION**

Even though the low corrosion resistance is a limitation for the broader use of magnesium in engineering applications, it is used in industry for its excellent strength to weight ratio [1-3]. Casting magnesium has considerable disadvantages as element segregation in the ingot during cooling is unavoidable, and some elements and compounds are insoluble in magnesium, even in the liquid form [4,5]. Magnesium strengthening can also be achieved by grain refinement, usually achieved by Severe Plastic Deformation (SPD) methods or powder metallurgy. This method offers the possibility of producing new alloys and composites, which are otherwise impossible to produce by conventional methods [6,7]. Due to favourable mechanical properties and corrosion resistivity, magnesium alloys are mainly used in engineering practice. Unalloyed Mg can provide benefits due to its purity highly demanded in the medical field.

Spark Plasma Sintering (SPS) allows fast consolidation of powder materials. This method effectively consolidates powders in short times due to rapid heating while a compressive load is applied [8-10]. The spark plasma sintering combines electrical energy with unidirectional mechanical pressure to convert powders into compacted material of the required dimensions and density. Typical pressures used for compacting during the SPS process range from 10 MPa to 100 MPa [11-13], even though some extremes reach up to 1 GPa [3]. The rapid heating is caused by Joule heating, which results from the electric current passing through the sintered material. The high electrical resistivity of the powder causes heating within the material, and no additional heating of the furnace is required [14]. Plastic flow significantly contributes to the pore closure, increasing the

overall sintering rate. As a result, a high density of the compacts can be achieved in short times or at a lower temperature than without applied current [15-17]. Typical sintering times for SPS methods are under 10 min [18], whereas hot pressing methods require much longer sintering times of 60 or more minutes [19]. A compacted material with good particle bonding and minimal metallic grain growth can be achieved. The main factor in the acceleration of the metal sintering process is the effect of disruption or evaporation of the oxide layer on the surface of powder [9,20].

In the literature, the pressure applied during SPS processing of pure magnesium varies from 30 MPa to 100 MPa. This study, therefore, focuses on the estimation of the influence of applied compacting pressure during SPS when processing pure Mg.

## 2. EXPERIMENTAL PART

The magnesium powder with 27.6  $\mu\text{m}$  average particle size was used to prepare all experimental materials. The measurement revealed homogenous particle size distribution with an average particle size with modulus 32.9  $\mu\text{m}$  and median 26.4  $\mu\text{m}$ . The chemical composition, size, and shape of the used powder particles were verified using ZEISS EVO LS 10 scanning electron microscope (SEM) with an energy dispersion analyser (EDS). The elemental analysis confirmed the declared purity of magnesium (Mg powder was supplied by Goodfellow company, declared purity was 99.7 %). The purity refers to metallic inclusions; however, the surface of the particles was oxidised for safety during transport. The powder particles were in the form of small chips. Magnesium powder was inserted into a steel die between two steel pistons, and uniaxial pressure of 100 MPa was applied to produce cylindrical green compacts 20 mm in diameter and approximately 5 mm in height. The amount of powder used for a single compact was 2.7 g. The green compacts (used for sintering) were prepared at room temperature.

The green compacts were inserted into a graphite die between two graphite pistons. The die was placed in the SPS chamber, which was closed and evacuated. After reaching a low vacuum of approximately 10 Pa, the electric power supply started the heating (Joule heating). The pressure of 5 MPa was applied to the inserted green compact during the chamber evacuation and temperature increase. The increase in temperature was set to 50  $^{\circ}\text{C}\cdot\text{min}^{-1}$ . After reaching 400  $^{\circ}\text{C}$ , additional compaction started at a 20  $\text{MPa}\cdot\text{min}^{-1}$  rate up to the selected pressure (20, 40, 60, 80 and 100 MPa). The heating at the selected pressure was set to 10 min. The prepared experimental materials were cooled in the evacuated chamber.

The experimental materials were embedded in epoxy resin (metallographic specimen), ground and polished using a Tegramin-25 automatic grinder/polisher. The composite grinding wheels with a grain size from 220 to 4000 were used for the metallographic specimens grinding. The polishing was performed on polishing cloths with diamond pastes with a mean particle size of 3  $\mu\text{m}$  and 1  $\mu\text{m}$ . Isopropanol was used as a wetting agent and rinse to minimise the oxidation of metallographic specimens during the metallographic preparation. The metallographic evaluation was performed using SEM. The porosity was calculated from the dimensions and mass of the individual sintered compacts. The microstructure evaluation by electron backscatter diffraction (EBSD) was performed on polished and etched metallographic cross-cut sections of four selected SPS samples using a Jeol JSM 7600F SEM. High angle grain boundaries were determined according to a misorientation of 15 $^{\circ}$ . The accelerating voltage was set to 20 kV for the best signal to noise ratio.

## 3. RESULTS AND DISCUSSION

The typical microstructure of the experimental material is shown in **Figure 1**. No metallic grain boundaries within the powder particles can be seen on the etched metallographic specimens (**Figure 1**). The powder particle boundaries are observable due to the presence of the oxide layer. The oxides are common on powder particle boundaries of magnesium [21]. A thin uniform layer of magnesium oxide was present on the surface of the powder particles even before the compaction because the manufacturer intentionally oxidised the

powder particles for safer transportation. Some oxidation can be related to the preparation and etching of metallographic specimens.

The SEM observation of etched metallographic specimens clearly shows the highest porosity of the experimental material prepared at the lowest (20 MPa) compacting pressure (**Figure 1a**). It is the same level of porosity as for the original green compact [22]; therefore, 20 MPa load during the SPS does not contribute to the compaction of the green compact. With the increase of compacting pressure during SPS, the porosity in experimental materials continually decreases to an apparent minimum of 5 % (for 80 MPa). This decrease can be attributed mainly to the pore closure due to the combined effect of sintering temperature and sintering pressure.

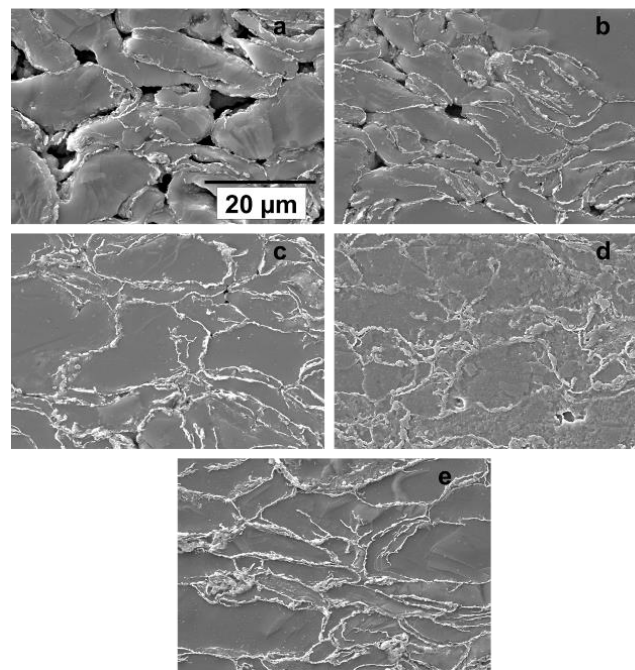


**Figure 1** The etched (2% Nital) microstructure of sintered compacts; a) 20 MPa during SPS; b) 40 MPa during SPS; c) 60 MPa during SPS; d) 80 MPa during SPS; e) 100 MPa during SPS

A higher temperature during sintering is connected with the higher plasticity of magnesium due to the activation of more slip systems, allowing plastic deformation in the magnesium hcp structure [23,24] to occur. Also, sufficient pressure has to be applied. Based on the obtained results, at least 40 MPa of compacting pressure should be applied during the sintering of green compacts to decrease the porosity of the experimental materials.

Compared to the microstructure of the experimental materials prepared at lower (below 60 MPa) pressures, the microstructure of the experimental materials prepared at higher compaction pressures (at and above 80 MPa) consists of highly deformed powder particles. Besides the plastic deformation of magnesium, the used pressure must be high enough to break the oxide layer created on the particle surface, resulting in accelerated diffusion. The EBSD method revealed significant changes in the microstructure of the experimental materials. Materials sintered at 40 MPa and 60 MPa revealed connected oxide layers on the powder particle boundaries (dark areas - areas not indexed by EBSD containing high amount of oxygen). Increasing the pressure during sintering led to powder particle connection (**Figures 2c** and **d**). The material sintered at the highest compacting pressure (100 MPa) contains only small areas of closed porosity (**Figure 2d**). A similar microstructure was found for magnesium material sintered at 390 °C under 90 MPa compacting pressure presented in [25].

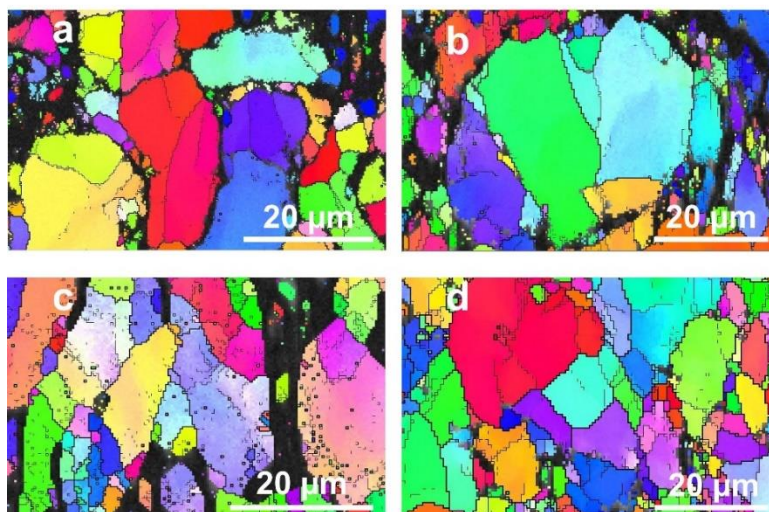


**Figure 2** IPF of sintered materials; a) 40 MPa during SPS; b) 60 MPa during SPS; c) 80 MPa during SPS; d) 100 MPa during SPS

The original green compacts used for sintering contain many interconnected pores, which means that the material contains only a limited amount of contact points between the powder particles. These pores remain open during the sintering at low compacting pressure (below 40 MPa), resulting in highly porous experimental materials. Thus, for low compacting pressures, the SPS technique has only minimal effect on the final porosity. Due to the increased compacting pressure during sintering, the open porosity changed to a closed porosity, and its amount decreased.

The density calculation from the dimensions and the weight of the experimental material also confirmed porosity levels. The results are shown in **Table 1**.

**Table 1** Calculated porosity of experimental materials (initial porosity of green compacts was 24 %)

Compacting pressure during SPS (MPa)	Porosity (%)
20	24 ± 1
40	12 ± 1
60	8 ± 1
80	5 ± 1
100	6 ± 1

#### 4. CONCLUSION

The green magnesium compacts prepared at room temperature applying 100 MPa for 60 s were sintered using the SPS method at 400 °C for 10 min with varying additional compacting pressures (20, 40, 60, 80 and 100 MPa). The compacting pressure during sintering significantly affected the resulting experimental material properties.

- The microstructure of the prepared experimental materials strongly depends on the applied pressure during sintering. With increasing compacting pressure, the porosity of the experimental materials continually decreased from 24 % to approximately 5 %.

- The compacting pressure of at least 80 MPa should be used to sufficiently bond magnesium powder particles during SPS at 400 °C when sintering green compacts.

## ACKNOWLEDGEMENTS

***This work was supported by Specific University Research at FCH BUT, Project Nr. FCH-S-22-8012, Ministry of Education, Youth and Sports of the Czech Republic.***

## REFERENCES

- [1] IBRAHIM, H., KLARNER, A.D., POORGANJI, B., DEAN, D., LUO, A.A., ELAHINIA, M. Microstructural, mechanical and corrosion characteristics of heat-treated Mg-1.2Zn-0.5Ca (wt%) alloy for use as resorbable bone fixation material. *J. Mech. Behav. Biomed. Mater.* 2017, vol. 69, pp. 203-212.
- [2] KUBÁSEK, J., DVORSKÝ, D., ČAVOJSKÝ, M., VOJTĚCH, D., BERONSKÁ, N., FOUISOVÁ, M. Superior properties of Mg-4Y-3RE-Zr alloy prepared by powder metallurgy. *J. Mater. Sci. Technol.* 2017, vol. 33, pp. 652-660.
- [3] KHAN, M.U.F., PATIL, A., CHRISTUDASJUSTUS, J., BORKAR, T., GUPTA, R.K. Spark plasma sintering of a high-energy ball milled Mg-10 wt% Al alloy. *J. Magnes. Alloy.* 2020, vol. 8, pp. 319-328.
- [4] ÇAKMAK, G., KÁROLY, Z., MOHAI, I., ÖZTÜRK, T., SZÉPVÖLGYI, J. The processing of Mg-Ti for hydrogen storage. Mechanical milling and plasma synthesis. *Int. J. Hydrogen Energy.* 2010, vol. 35, pp. 10412-10418.
- [5] KONDOH, K., FUKUDA, H., UMEDA, J., IMAI, H., FUGETSU, B., ENDO, M. Microstructural and mechanical analysis of carbon nanotube reinforced magnesium alloy powder composites. *Mater. Sci. Eng. A.* 2010, vol. 527, pp. 4103-4108.
- [6] HASSAN, S.F., GUPTA, M. Development of ductile magnesium composite materials using titanium as reinforcement. *J. Alloys Compd.* 2002, vol. 345, pp. 246-251.
- [7] CHIANE, V.A., HOSSEINI, H.R.M., NOFAR, M. Microstructural features and mechanical properties of Al - Al<sub>3</sub>Ti composite fabricated by in-situ powder metallurgy route. *Materials&Design.* 2009, vol. 473, pp. 127-132.
- [8] MONDET, M., BARRAUD, E., LEMONNIER, S., ALLAIN, N., GROSDIDIER, T. Optimisation of the mechanical properties of a Spark Plasma Sintered (SPS) magnesium alloy through a post-sintering in-situ precipitation treatment. *J. Alloys Compd.* 2017, vol. 698, pp. 259-266.
- [9] PARASKEVAS, D., DADBAKSH, S., VLEUGELS, J., VANMEENSEL, K., DEWULF, W., DUFLOU, J.R. Solid state recycling of pure Mg and AZ31 Mg machining chips via spark plasma sintering. *Mater. Des.* 2016, vol. 109, pp. 520-529.
- [10] MINÁRIK, P., ZEMKOVÁ, M., LUKÁČ, F., BOHLEN, J., KNAPEK, M., KRÁL, R. Microstructure of the novel biomedical Mg-4Y-3Nd alloy prepared by spark plasma sintering. *J. Alloys Compd.* 2020, vol. 819.
- [11] DVORSKÝ, D., KUBÁSEK, J., PRŮŠA, F., KRISTIANOVÁ, E., VOJTĚCH, D. Specific interface prepared by the SPS of chemically treated Mg-based powder. *Mater. Chem. Phys.* 2021, vol. 261.
- [12] CUI, Z., LI, W., CHENG, L., GONG, D., CHENG, W., WANG, W.: Effect of nano-HA content on the mechanical properties, degradation and biocompatible behavior of Mg-Zn/HA composite prepared by spark plasma sintering. *Mater. Charact.* 2019, vol. 151, pp. 620-631.
- [13] SODERLIND, J., CIHOVA, M., SCHÄUBLIN, R., RISBUD, S., LÖFFLER, J.F. Towards refining microstructures of biodegradable magnesium alloy WE43 by spark plasma sintering. *Acta Biomater.* 2019, vol. 98, pp.67-80.
- [14] ZHANG, Z.-H., LIU, Z.-F., LU, J.-F., SHEN, X.-B., WANG, F.-C., WANG, Y.-D. The sintering mechanism in spark plasma sintering - Proof of the occurrence of spark discharge. *Scr. Mater.* 2014, vol. 81, pp. 56-59.
- [15] SUÁREZ, M., FERNÁNDEZ, A., MENÉNDEZ, J. Challenges and opportunities for spark plasma sintering: A Key technology for a new generation of materials. *Sinter. Appl.* 2013, p. 319.
- [16] ČAPEK, J., VOJTĚCH, D. Characterization of porous magnesium prepared by powder metallurgy - influence of powder shape. *Manuf. Technol.* 2014, vol. 14, pp. 271-275.

- [17] DVORSKY, D., KUBASEK, J., JABLONSKA, E., KAUFMANOVA, J., VOJTECH, D. Mechanical, corrosion and biological properties of advanced biodegradable Mg-MgF<sub>2</sub> and WE43-MgF<sub>2</sub> composite materials prepared by spark plasma sintering. *J. Alloys Compd.* 2020, vol. 825, p. 154016.
- [18] KNAPEK, M., ZEMKOVÁ, M., GREŠ, A., JABLONSKÁ, E., LUKÁČ, F., KRÁL, R., BOHLEN, J., MINÁRIK, P. Corrosion and mechanical properties of a novel biomedical WN43 magnesium alloy prepared by spark plasma sintering. *J. Magnes. Alloy.* 2021, vol. 9, pp. 853-865.
- [19] TURAN, M.E., SUN, Y., AKGUL, Y. Mechanical, tribological and corrosion properties of fullerene reinforced magnesium matrix composites fabricated by semi powder metallurgy. *J. Alloys Compd.* 2018, vol. 740, pp. 1149-1158.
- [20] UMEDA, J., KONDOH, K., KAWAKAMI, M., IMAI, H. Powder metallurgy magnesium composite with magnesium silicide in using rice husk silica particles. *Powder Technol.* 2009, vol. 189, pp. 399-403.
- [21] LEE, C.S., LEE, H.C., KIM, G., HAN, J.H., KIM, W.J., KIM, H.S. Design of Mg-6wt%Al alloy with high toughness and corrosion resistance prepared by mechanical alloying and spark plasma sintering. *Mater. Charact.* 2019, vol. 158, p. 109995.
- [22] BŘEZINA, M., DOLEŽAL, P., KRYSTÝNOVÁ, M., MINDA, J., ZAPLETAL, J., FINTOVÁ, S., WASSERBAUER, J. Evolution of microstructure and electrochemical corrosion characteristics of cold compacted magnesium. *Koroze a Ochr. Mater.* 2017, vol. 61.
- [23] CHAPUIS, A., DRIVER, J.H. Temperature dependency of slip and twinning in plane strain compressed magnesium single crystals. *Acta Mater.*, 2011, vol. 59, pp. 1986-1994.
- [24] TANE, M., MAYAMA, T., ODA, A., NAKAJIMA, H. Effect of crystallographic texture on mechanical properties in porous magnesium with oriented cylindrical pores. *Acta Mater.* 2015, vol. 84, pp. 80-94.
- [25] WANG, X., JIANG, L., ZHANG, D., RUPERT, T.J., BEYERLEIN, I.J., MAHAJAN, S., LAVERNIA, E.J., SCHOENUNG, J.M. Revealing the deformation mechanisms for room-temperature compressive superplasticity in nanocrystalline magnesium. *Materialia.* 2020, vol. 11, p.100731.